SimeXmin
XI SIMPÓSIO BRASILEIRO DE EXPLORAÇÃO MINERAL
XI BRAZILIAN SYMPOSIUM ON MINERAL EXPLORATION

Ore-forming Systems of the Volta Grande Gold Deposit (World Class), Bacaja Domain, Amazon Craton.

Hugo Paiva Tavares de Souza
ANM

Mineral Resources

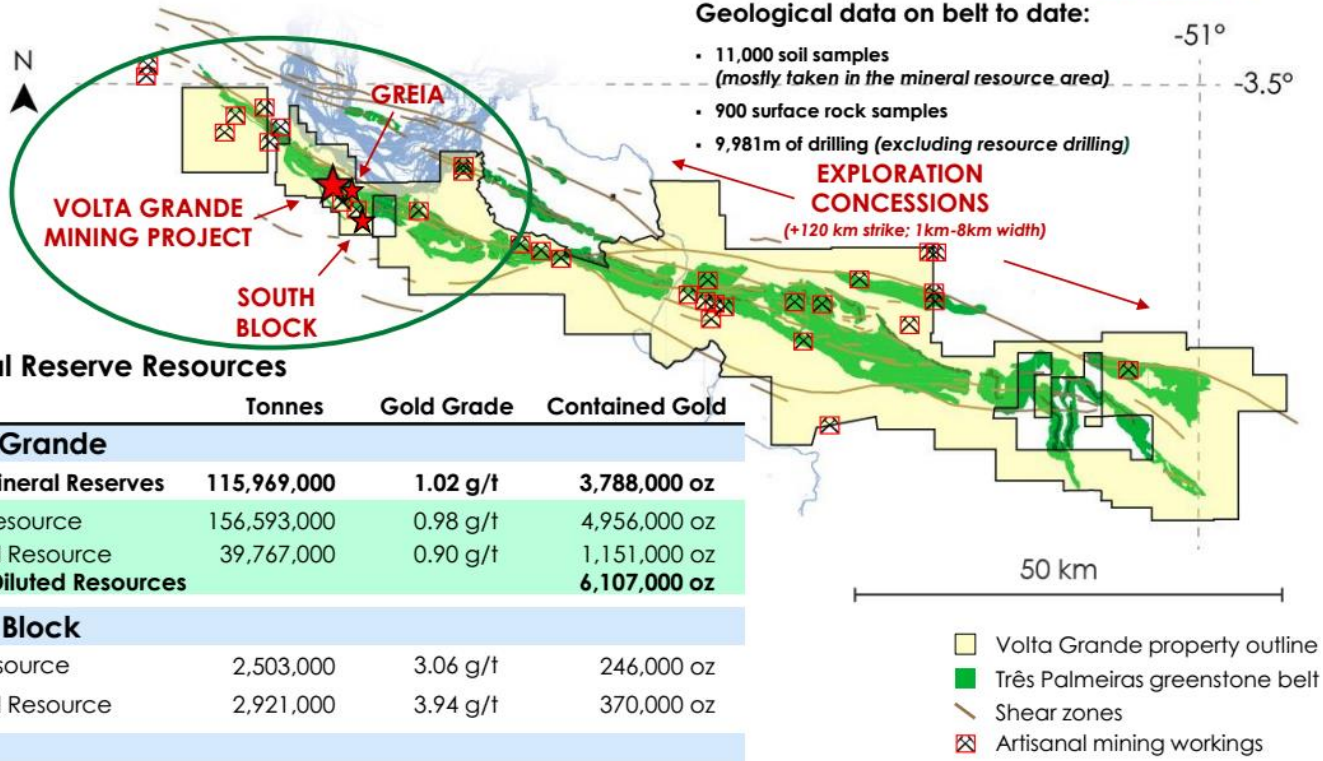

Mineral Reserve Resources

	Tonnes	Gold Grade	Contained Gold
Volta Grande			
P & P Mineral Reserves	**115,969,000**	**1.02 g/t**	**3,788,000 oz**
M & I Resource	156,593,000	0.98 g/t	4,956,000 oz
Inferred Resource	39,767,000	0.90 g/t	1,151,000 oz
TOTAL Diluted Resources			**6,107,000 oz**
South Block			
M&I Resource	2,503,000	3.06 g/t	246,000 oz
Inferred Resource	2,921,000	3.94 g/t	370,000 oz
Greia			
Inferred Resource	2,020,000	1.79 g/t	115,000 oz

Fig. 1 - Mineral Resources, Belo Sun Mining 2019.

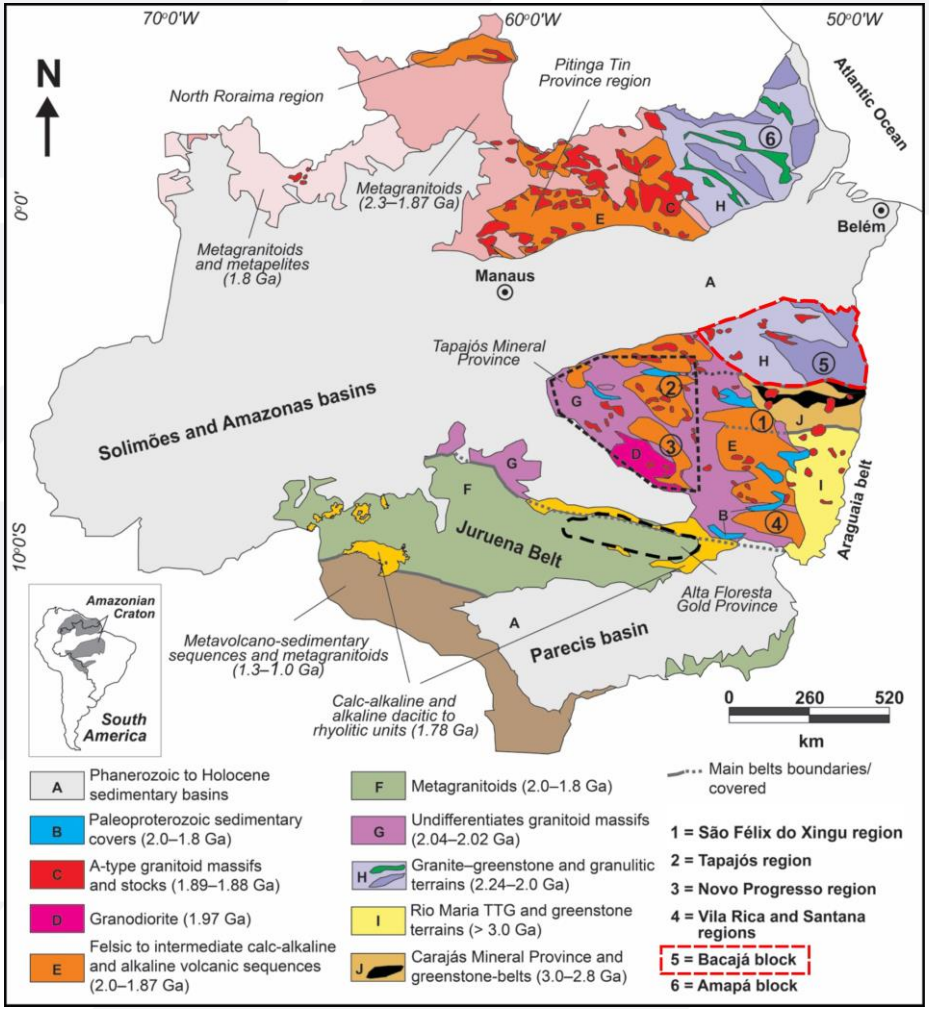

Fig. 2 – Simplefield geological map of the Amazon Craton, Fernandes and Juliani, 2019.

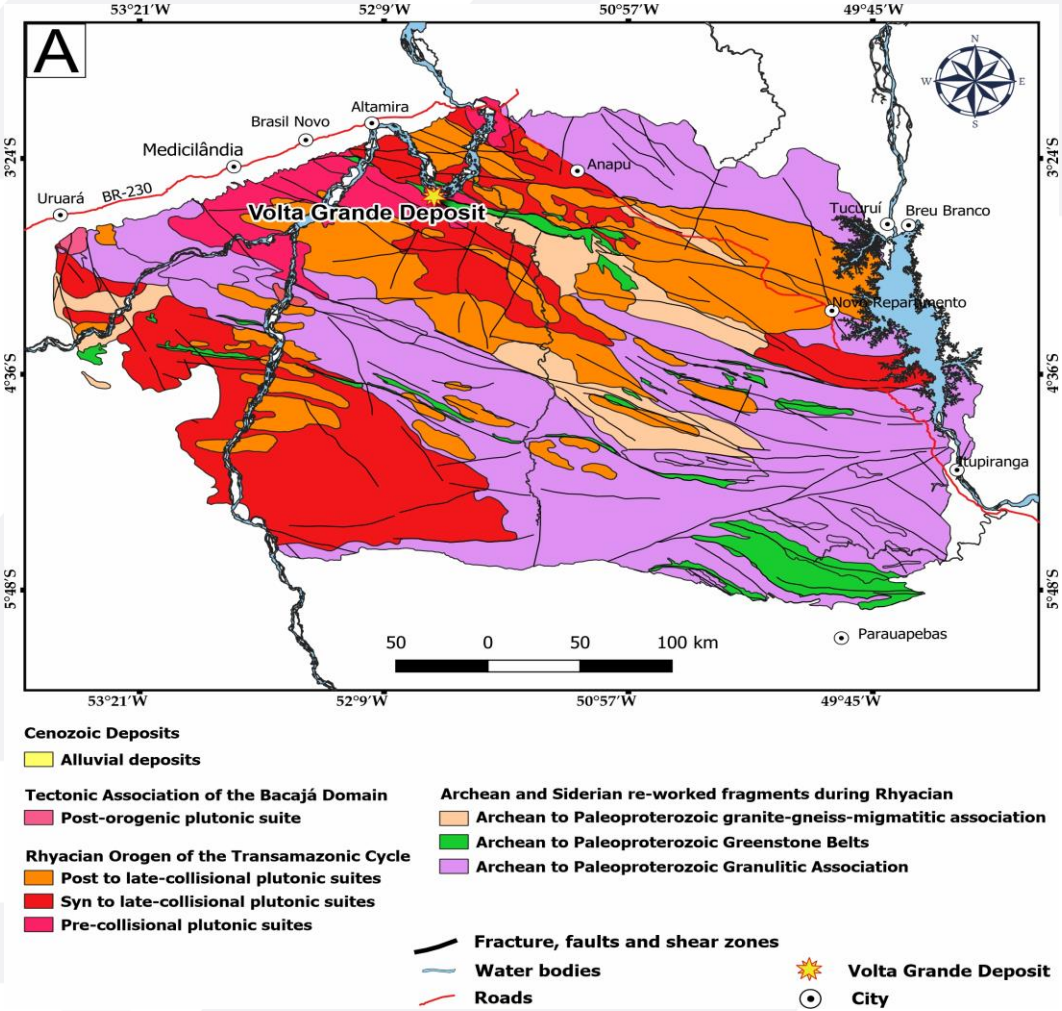

Fig. 3 - Regional geological map of the Bacaja Domain, Vasquez et al., 2008b.

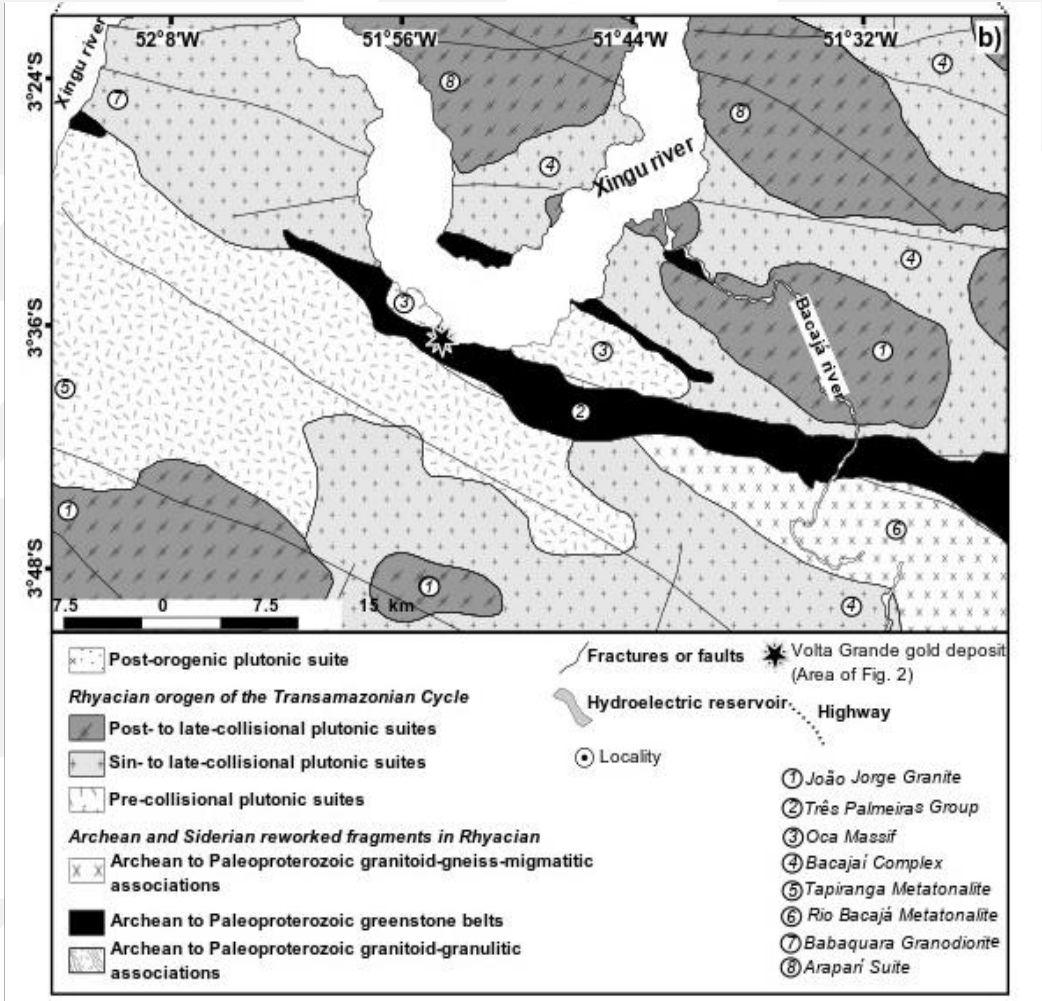

Fig. 4 - Detail of the previous geological map for the dominant host units of the Volta Grande gold deposit (black star) and neighboring units (Vasquez et al., 2008c).

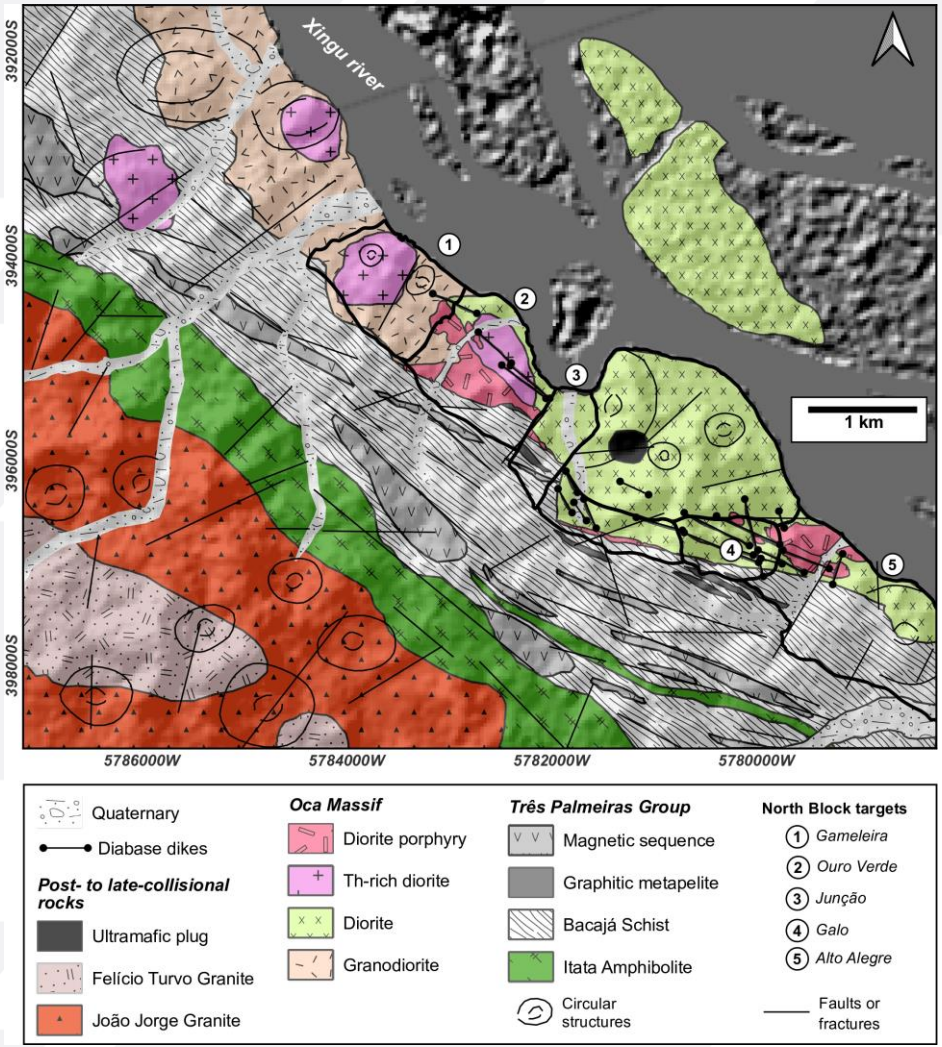

Fig. 5 - Overlay of the geological map (supplied by Belo Sun Mining Corp) and the hillshade model based on a Shuttle radar topographic mission image (Farr and Kobrick, 2000) of the Volta Grande gold deposit. The dotted polygon shows high-grade ore-bearing targets (1–5) of the North block.

SimeXmin
XI SIMPÓSIO BRASILEIRO DE EXPLORAÇÃO MINERAL
XI BRAZILIAN SYMPOSIUM ON MINERAL EXPLORATION

Methods

One hundred and twenty-one described rock samples represent five drilling holes named Gameleira (M01/VVGD-391), Ouro Verde M02/VVGD-359), Junção (M03/VVGD-674), Galo (M04/VVGD-145), and Alto Alegre (M05/VVD-145) that are promising exploitation targets in the North block.

Mesoscopic descriptions of fifty-five thin sections revealed several lithologies associated with the ore-forming processes and guided the microscopic investigation under transmitted and reflected light aiming the metallogenetic interpretation. Ore minerals identification and classification of volcanic, plutonic, and metamorphic lithotypes.

Scanning electron microscopy (SEM) analyzes were conducted on the EVO LS15 microscope of the Zeiss

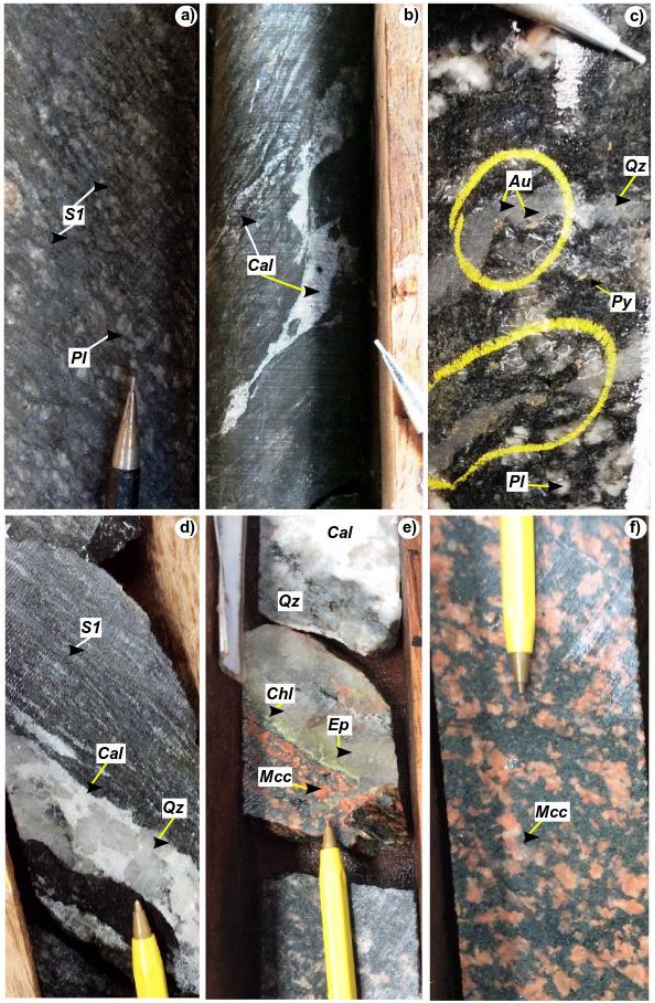

Fig. 6 - **a)** mylonitic granodioritic gneiss with plagioclase (Pl) porphyroclasts;
b) carbonate alteration with calcite (Cal) controlled by S1 foliation in metaandesite;
c) visible gold and sulfides in quartz (Qz) veins with in mylonitic granodiorite;
d) quartz (Qz) and calcite (Cal) veins in mylonitized amphibolite. Note the S1-controlled carbonate alteration;
e) quartz (Qz) and calcite (Cal) vein associated with reddish mylonitic granodiorite with selective potassic alteration (Mcc). Note the superposition of propylitic alteration related to epidote (Ep) and chlorite (Chl);
f) reddish mylonitic granodiorite with selective potassic alteration (Mcc).

Fig. 7 - a) monzodiorite with flow-related foliation and plagioclase (Pl), Ca-amphibole (Hbl) and biotite (Bt);
b) porphyritic dacite (top) with flow-oriented plagioclase phenocrysts (Pl) and aphyric groundmass in contact with foliated porphyritic granodiorite (bottom);
c) microgranite with biotite (Bt), secondary hydrothermal microcline (Mcc), and associated quartz (Qz) veins. Note selective propylitic alteration with epidote (Ep) and chlorite (Chl);
d) porphyritic rhyodacite revealing selective potassic alteration with microcline (Mcc) phenocrysts and later fracture-controlled propylitic alteration with epidote (Ep) and chlorite (Chl);
e) gold particles with in stockwork silicification (Qz) zone with adularia (Adu) and associated hydrothermal breccia;
f) potassic alteration with microcline (Mcc) on quartz monzodiorite.


A
V.G

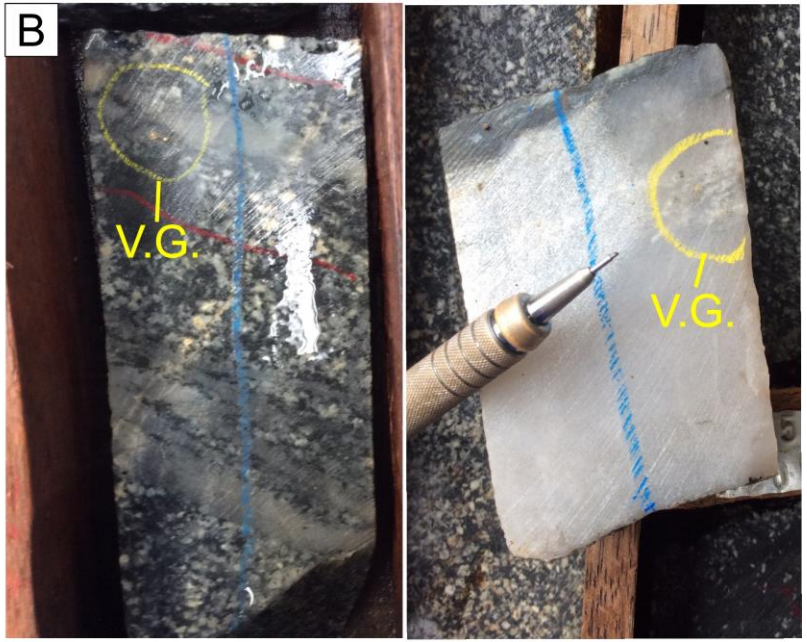
B
V.G.
V.G.

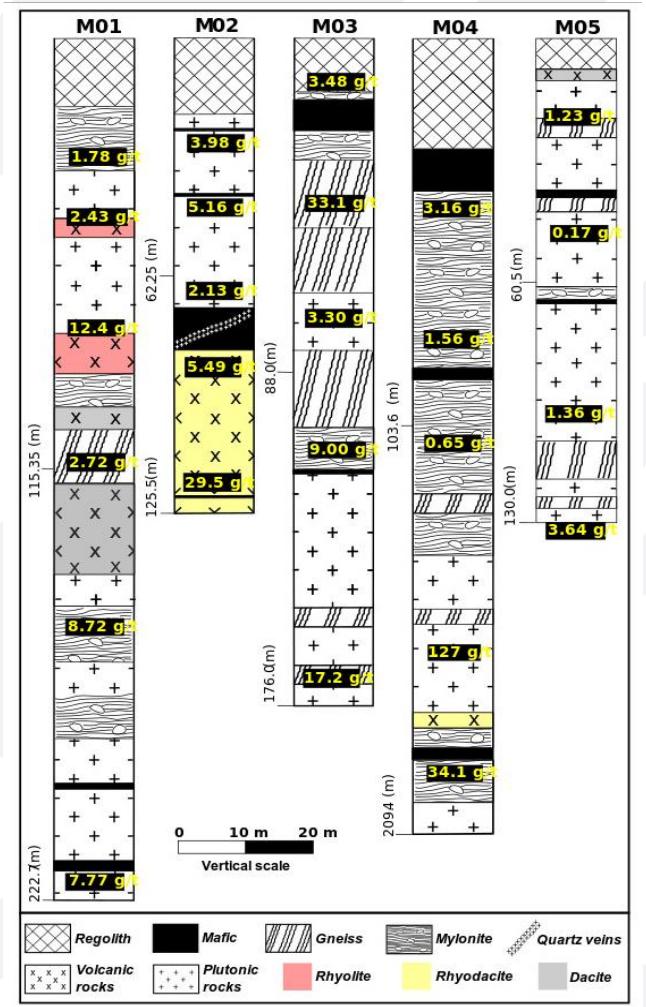

Mylonite, gneiss and associated metamafic rocks that underwent greenschist to amphybolite-facies metamorphism.

Quartz monzonite, granodiorite, monzodiorite, quartz monzodiorito, subordinate microgranite and volcanics crosscutting the older metamorphic rocks.

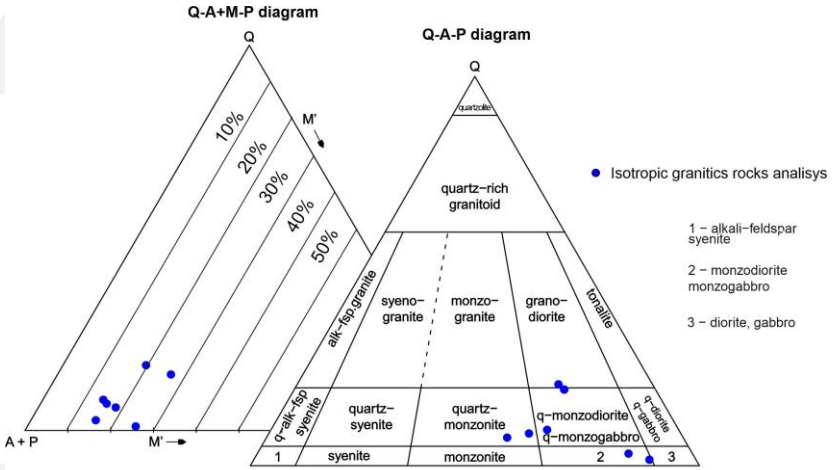

SimeXmin
XI SIMPÓSIO BRASILEIRO DE EXPLORAÇÃO MINERAL
XI BRAZILIAN SYMPOSIUM ON MINERAL EXPLORATION

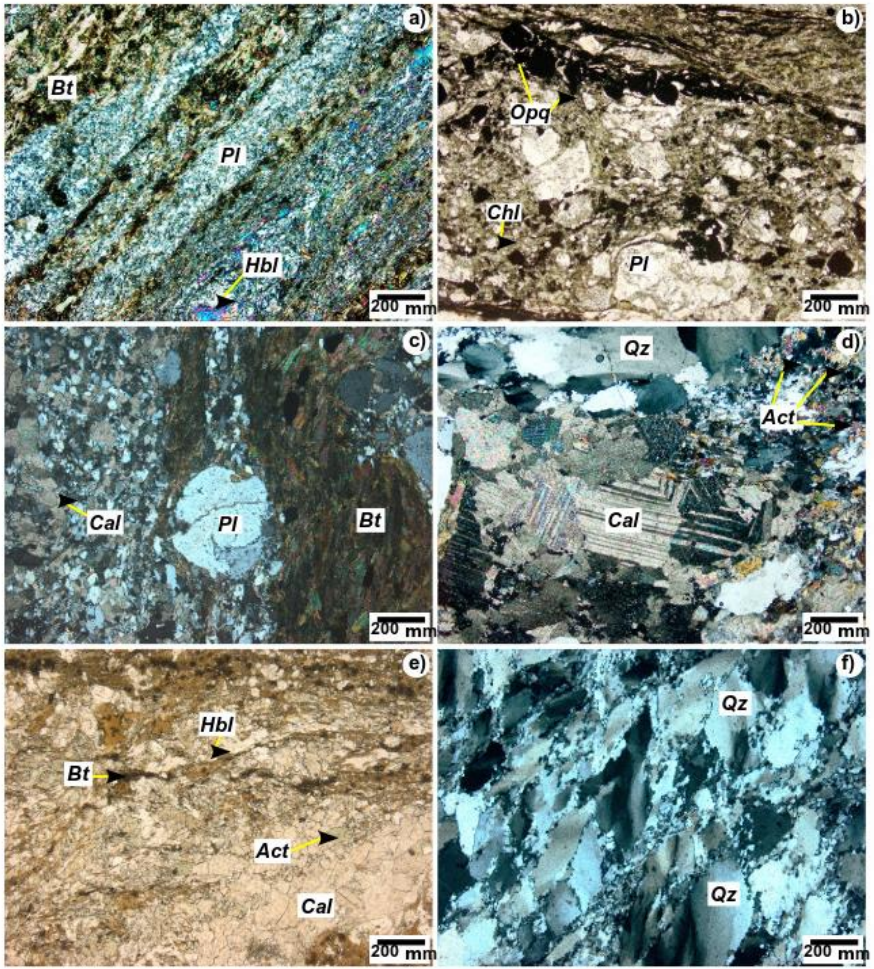

Fig. 10 - **a)** meta-andesite with felsic bands comprising fine-grained plagioclase (Pl) and mafic bands with Ca-amphibole (Hbl) and biotite (Bt).
b) mylonitic quartz monzodiorite showing plagioclase (Pl) porphyroclasts and Fe–Ti oxides (Opq). Note the dispersion of chlorite (Chl) related to selective propylitic alteration;
c) mylonitic granodiorite with plagioclase (Pl) porphyroclast and biotite (Bt). The groundmass contains quartz, plagioclase and calcite (Cal) of the pervasive carbonate alteration;
d) mylonitic granodiorite with calcite (Cal) of the carbonate alteration, Quartz (Qz) and retrograde metamorphic actinolite (Act);
e) retrograde metamorphic amphibolite calcite (Cal), Ca-amphibole (Hbl), secondary biotite (Bt) and actinolite (Act);
f) metamorphosed quartz (Qz).

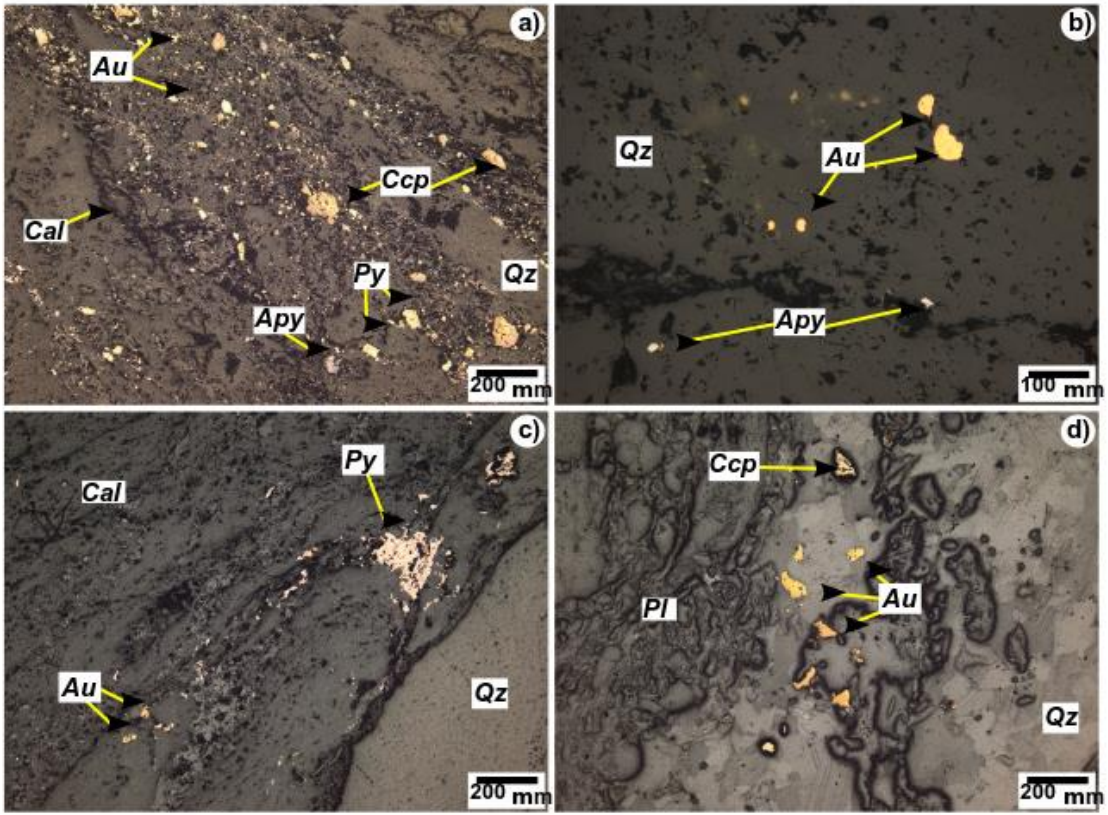

Fig. 11 - **a)** gold (Au), chalcopyrite (Ccp), pyrite (Py) and arsenopyrite (Apy) grains along the S1 foliation in mylonitic monzodiorite. Calcite (Cal) and quartz (Qz) are gangue;
b) gold (Au), arsenopyrite (Apy) particles in quartz (Qz) veins in mylonitic granodiorite.
c) pyrite (Py) aggregate and minor gold (Au) particles along calcite (Cal) and quartz (Qz) carbonat e alteration syn - chronous with the S1 foliation in amphibolite;
d) gold (Au), chalcopyrite (Ccp) in mylonitic quartzdiorite. Plagioclase (Pl) and quartz (Qz) are gangue.

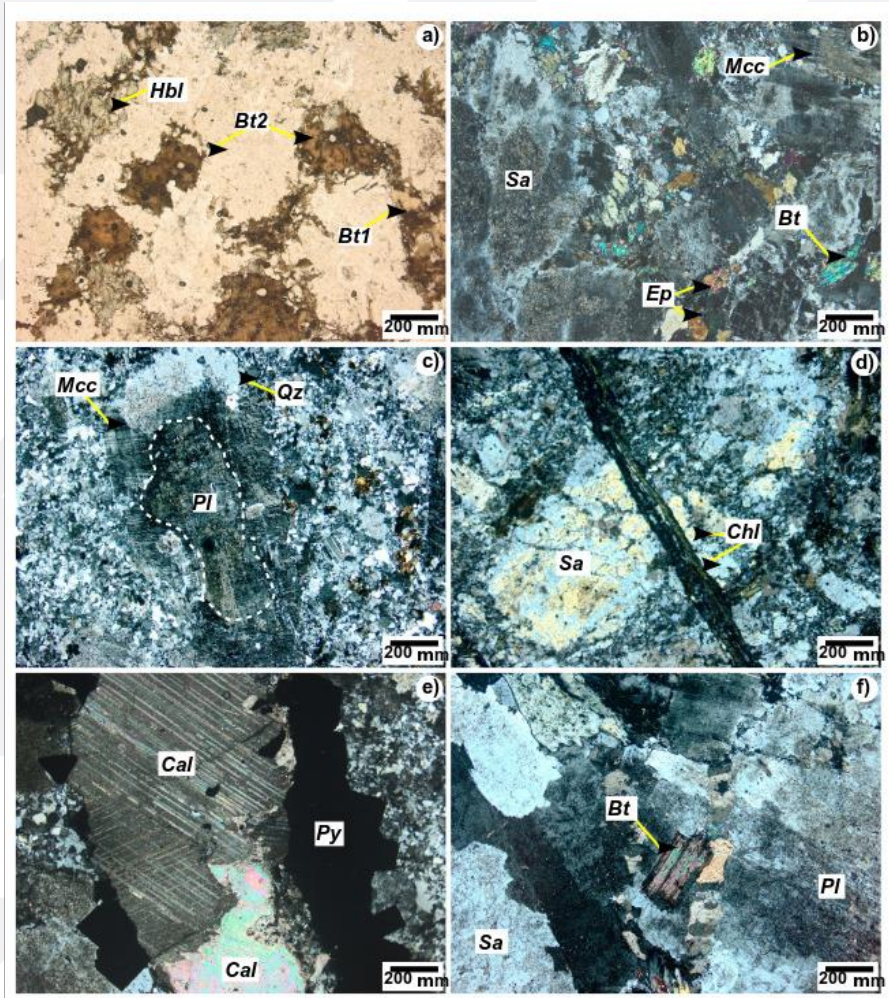

Fig. 12 - **a)** Ca-amphibole (Hbl), biotite (Bt1) microgranite and secondary biotite (Bt2) related to potassic alteration;
b) porphyritic rhyolite with sanidine (Sa) and biotite (Bt) in a felsophyric groundmass whith selective potassic alteration related to microcline (Mcc) replacing plagioclase and pervasive propylitic alteration with epidote (Ep);
c) porphyritic dacite with plagioclase (Pl) and minor quartz (Qz) phenocrysts in a microlithic groundmass.
d) sanidine (Sa) and felsophyric groundmass in porphyritic rhyodacite.
e) calcite (Cal) and pyrite (Py) grains related to fracture-controlled carbonate alteration in aphyric dacite with felsophyric groundmass;
f) quartz monzodiorite with sanidine (Sa), plagioclase (Pl), and minor chloritized biotite (Bt). The“dusty” aspect of feldspars is a product of sericitic alteration with fine-grained muscovite (Ms) and superimposed argillic alteration.

Fig. - 13 **a)** colloidal quartz along the stockwork system in porphyritic dacite;
b) platy calcite grains with comb texture along the stockwork system in porphyritic rhyolite
c) Gold (Au), chalcopyrite (Cal), and arsenopyrite (Apy) grains in quartz (Qtz) vein that composesa stockwork system in porphyritic dacite;
d) pyrite (Py) aggregate at the border of calcite (Cal) veinlet and quartz (Qz) groundmass in porphyritic rhyolite;
e) disseminated gold (Au) and pyrite (Py) grains in quartz monzodiorite. The gangue is quartz and feldspars;
f) detail of gold flakes dispersed in a quartz-rich stockwork system.

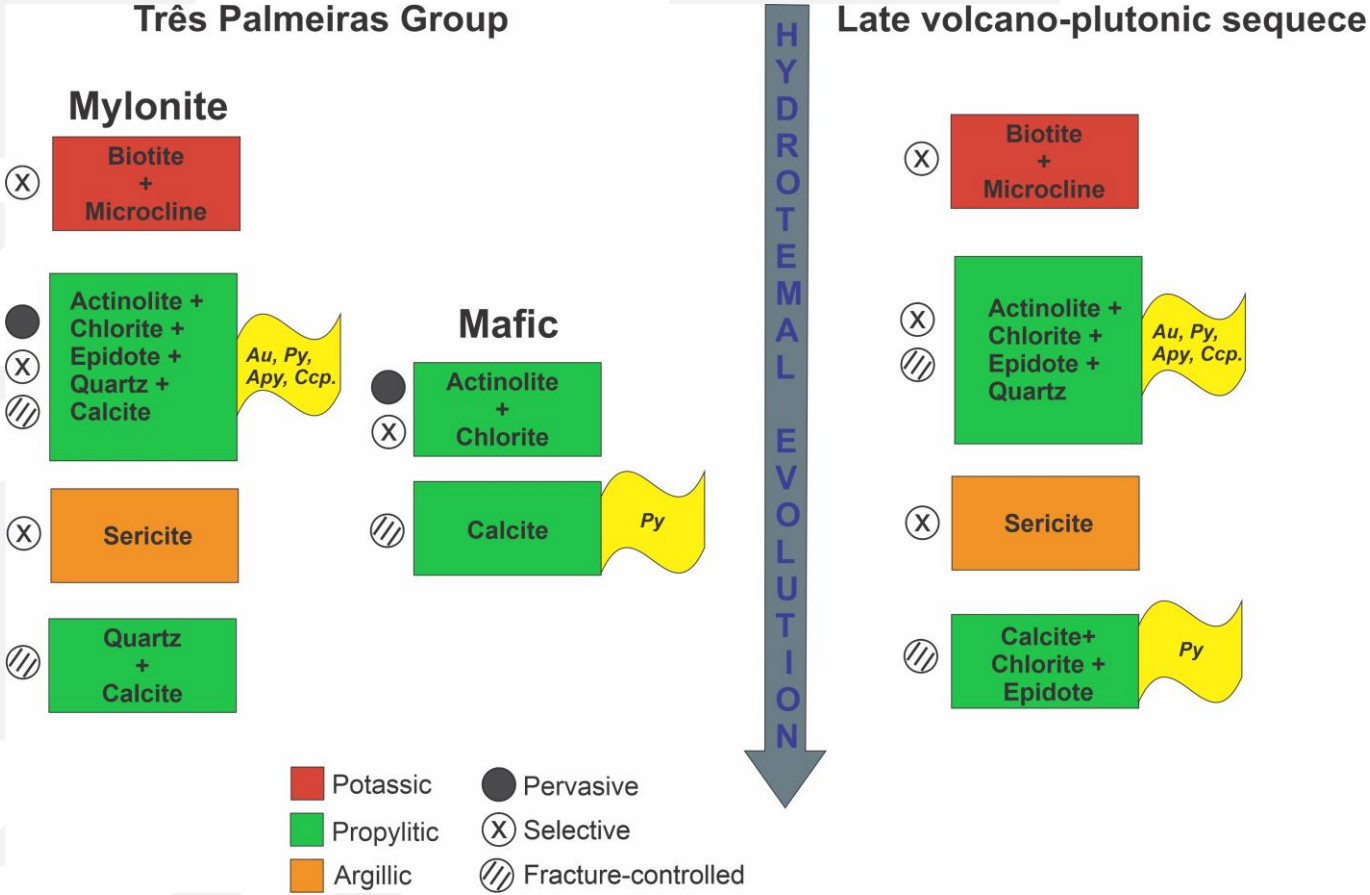

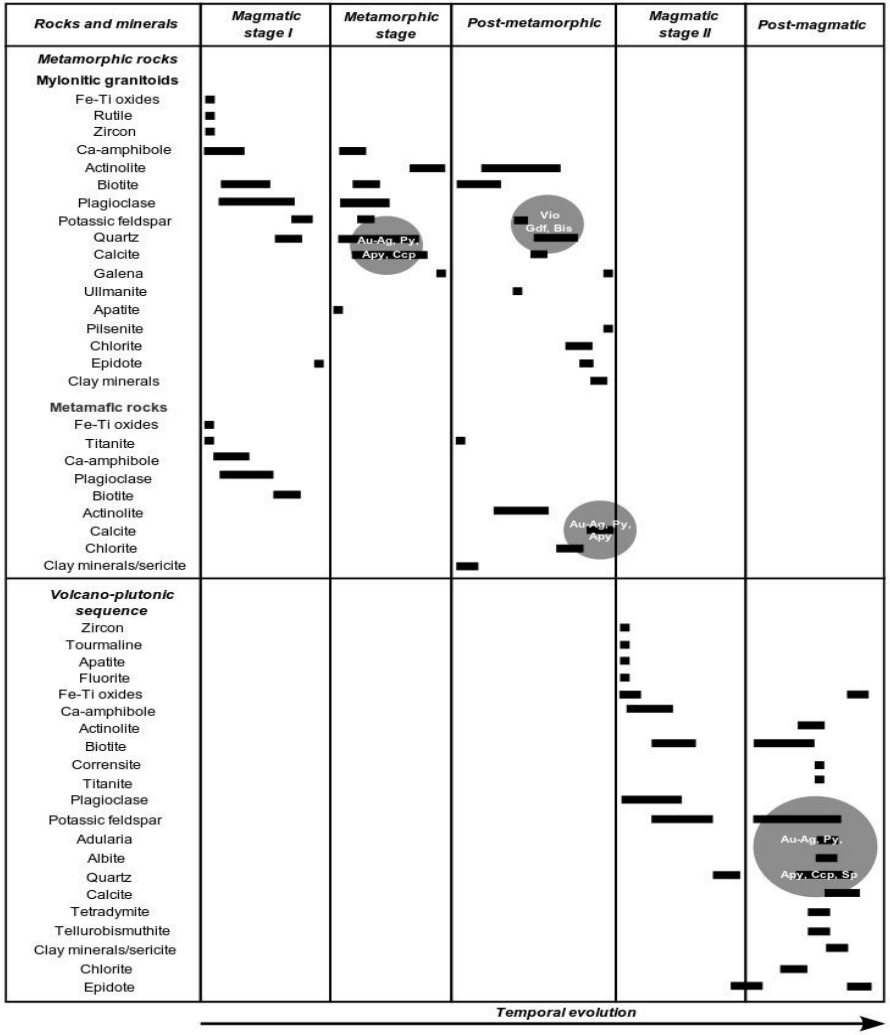

Fig. 15 - Metamorphism, hydrothermal alteration and interpreted paragenetic sequence of the representative core samples. The five stages of mineral formation and mineralization episodes (gray circles).

The temporal evolution and mineral replacing havea basis on an idealized evolutionary hydrothermal alteration sequence (Pirajno, 2009).

SimeXmin
XI SIMPÓSIO BRASILEIRO DE EXPLORAÇÃO MINERAL
XI BRAZILIAN SYMPOSIUM ON MINERAL EXPLORATION

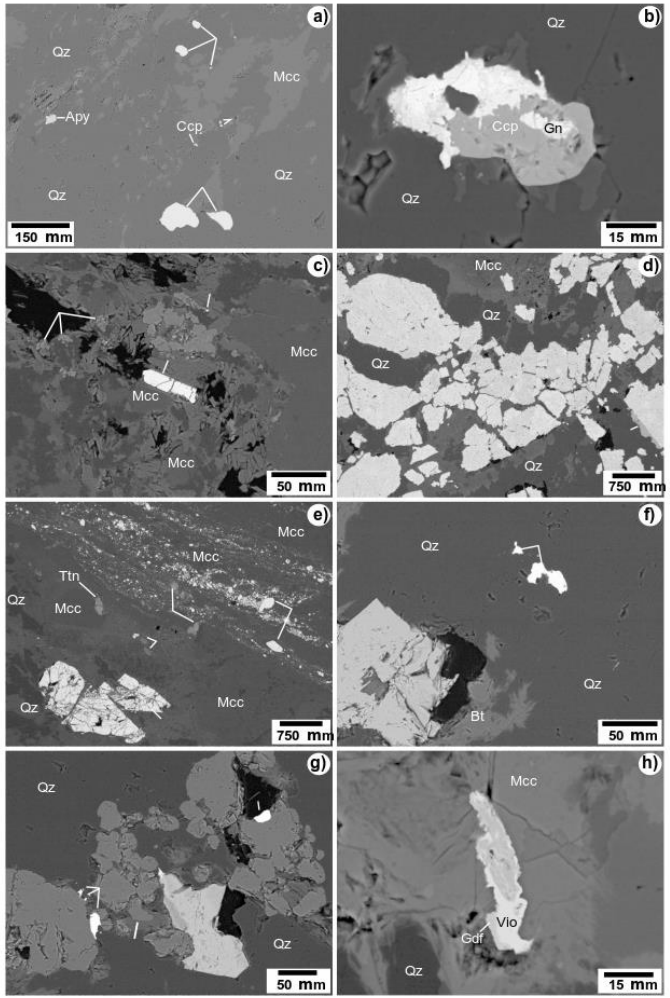

Fig. 16 - a) (Au–Ag), chalcopyrite (Ccp), and arsenopyrite (Apy) grains associated with quartz (Qz) and microcline (Mcc);
b) galena (Gn) inclusion replacing chalcopyrite (Ccp) in quartz (Qz) vein;
c) arsenopyrite (Apy), titanite (Ttn), zircon (Zrn), microcline (Mcc), and albite (Ab) related to potassic alteration;
d) arsenopyrite (Apy) and pyrite (Py) associated with quartz (Qz), calcite (Cal), and microcline (Mcc);
e) arsenopyrite (Apy), rutile (Rt), apatite (Ap), and titanite (Ttn) associated with microcline (Mcc) and quartz (Qz);
f) pyrite (Py), galena (Gn), and biotite (Bt) grains in quartz (Qz) veins related;
g) pyrite (Py), pilsenite (Pil), bismite (Bi), and apatite (Ap) associated with quartz (Qz) and clinochlore (Clc);
h) violarite (Vio) and gersdorffite (Gdf) at the border of ullmanite (Ull) associated with microcline (Mcc) and quartz (Qz) in fracture-controlled potassic alteration;

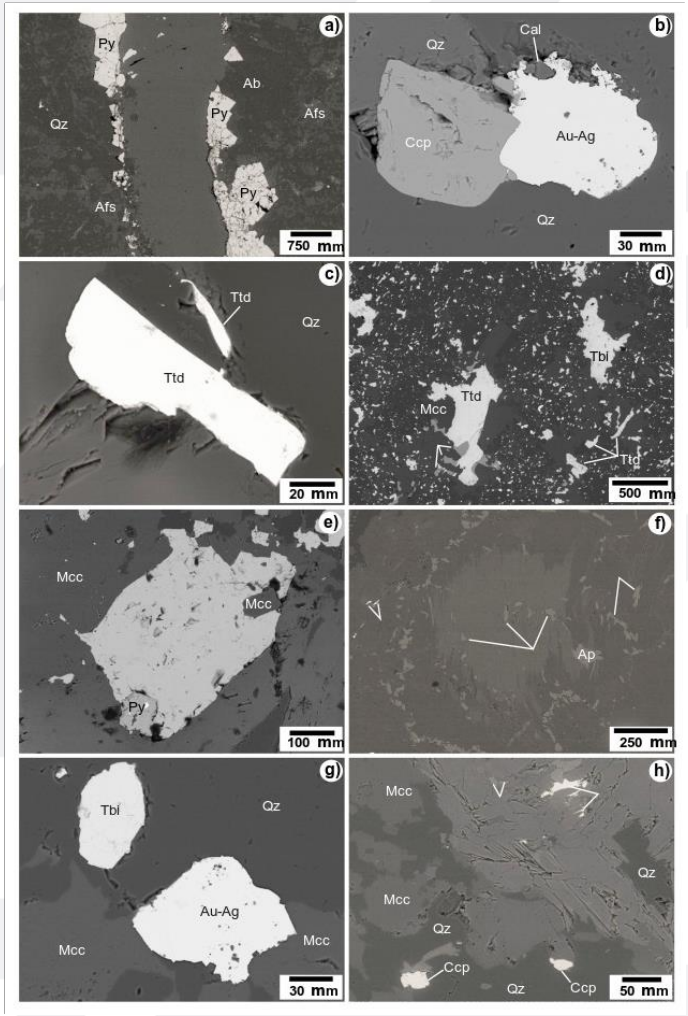

Fig. 16 - a) Pyrite (Py) and cal-cite (Cal) filling vein associated to quartz (Qz), adularia (Afs) and albite (Ab);
b) (Au–Ag) in contact with chalcopyrite(Ccp) grains disseminated in quartz (Qz) and minor calcite (Cal) vein;
c) vein with primary tetradymite (Ttd) grains, calcite (Cal), and quartz (Qz);
d) tellurobismuthite (Tbi) and tetradymite (Ttd) associated with microcline (Mcc), calcite (Cal), albite (Ab), and chalcopyrite (Ccp);
e) chalcopyrite (Ccp) and pyrite (Py) associated with potassic alteration with microcline (Mcc) and calcite (Cal);
f) corrensite (Corr) and actinolite (Act) at the border of biotite (Bt), chalcopyrite (Ccp) and secondary titanite (Ttn).
g) (Au–Ag) and tellurobismuthite (Tbi) grains associated with potassic alteration with microcline (Mcc) and quartz (Qz).
h) sphalerite (Sp) and chalcopyrite (Ccp) grains associated with actinolite (Act), microcline (Mcc), quartz (Qz), apatite (Ap) and titanite (Ttn).

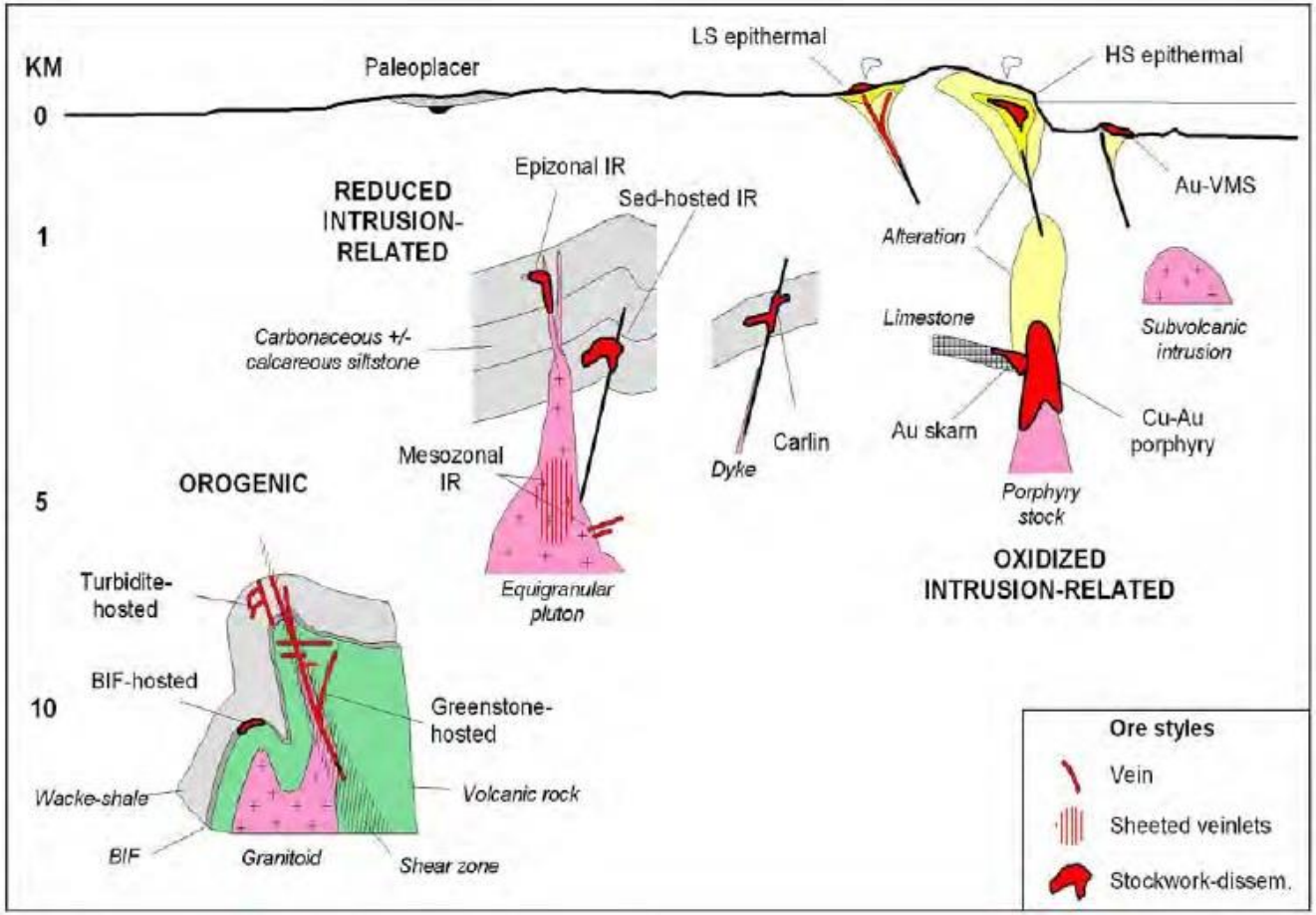

Fig. 17 - Schematic cross section showing the key geologic elements of the main gold systems and their crustal depths of emplacement. Modified from Poulsen *et al.*(2000), and Robert *et al.* (2004a)

Contents lists available at ScienceDirect

Journal of South American Earth Sciences

journal homepage: www.elsevier.com/locate/jsames

Multistage mineralizing episodes of the Proterozoic world-class Volta Grande gold deposit, Amazonian Craton, northern Brazil: Implications for the Bacajá Domain metallogenesis

Hugo Paiva Tavares de Souza [a], Carlos Marcello Dias Fernandes [a,*], Ricardo de Freitas Lopes [b], Stéphane Amireault [c], Raquel Souza da Cruz Saraiva [a], Brenda Gomes Silva Paresqui [a]

[a] Geosciences Institute, Federal University of Pará (UFPA), Rua Augusto Corrêa 1, Belém, PA, 66075-110, Brazil
[b] Ore Investments, R. Rio Grande do Norte 1435, Belo Horizonte, MG, 30130-131, Brazil
[c] Belo Sun Mining Corp., Toronto, ON M5H 2M5, Canada

ARTICLE INFO

Keywords:
Stratigraphy
Hydrothermal alteration
Orogenic gold
Volcanism-plutonism
Epithermal

ABSTRACT

The easternmost region of the Amazonian Craton in northern Brazil has been the focus of several mining exploration surveys, which led to the identification of the world-class Volta Grande gold deposit (~6.0 Moz@1.02 g/t). The deposit is inserted in the Bacajá Domain (2.24–2.0 Ga), and part of the mineralization occurs in Proterozoic mylonite, gneiss, and associated metamafic rocks that underwent greenschist to amphibolite-facies metamorphism. Electrum (Au–Ag) occurs as grains in cm-sized quartz high-grade veins and veinlets (up to 34.1 g/t in some rock intervals) that follow the mylonitic foliation and are associated with pervasive carbonate alteration, synchronous with the dynamic metamorphism. Disseminated electrum grains, pyrite, chalcopyrite, arsenopyrite, tellurides, and galena occur associated with potassic, argillic, propylitic, and silicic alteration types mainly in fracture-controlled or pervasive styles. These geological features as a whole suggest an orogenic high-tonnage orogenic gold system. Isotropic core samples along a stratigraphic profile reveal late andesite, dacite, rhyodacite, and rhyolite lava flows and dikes and plutonic rocks such as quartz monzonite, granodiorite, monzodiorite, and subordinate microgranite crosscutting the older metamorphic rocks. These rocks reveal potassic, propylitic, argillic, silicic, and sericitic alteration types. Electrum grains, possibly related to boiling deposition, occur along cm-sized quartz, calcite, and adularia high-grade veins (up to 29.5 g/t in some rock intervals) with chalcopyrite, pyrite, arsenopyrite, tetradymite, and tellurobismuthite. Such mineralogy is compatible with a low-sulfidation

Conclusion

i. The first mineralization event encompasses orthogneisses, mylonites, quartz veins, and local fracture-controlled pervasive carbonate formation. These rocks and minerals are products of tectonic-metamorphic processes in greenschist to amphibolite facies that caused the devolatilization process.

ii. A late mineralizing event is genetically associated with late intermediate to felsic isotropic volcanic and plutonic rocks. This volcano-plutonic sequence has large zones of stockwork texture with variable hydrothermal alteration types and styles, gold-bearing veins and venules with quartz, possibly adularia, sulfides, tellurides.

iii. The isotropic volcano-plutonic rocks and related circular structures in the Bacajá Domain have potentialities for new polymetallic mineralization discoveries, such as other Proterozoic terrains of the Amazonian Craton.

iv. We present a hypothesis regarding metallogenetic potential not described in the Bacajá Domain. The superimposition of mineralization events is primordial for an increase in their grade, tonnage, economic viability, and longevity.

SimeXmin
XI SIMPÓSIO BRASILEIRO DE EXPLORAÇÃO MINERAL
XI BRAZILIAN SYMPOSIUM ON MINERAL EXPLORATION

ANM

Obrigado

BELO SUN MINING

Hugo.souza@anm.gov.br

UNIVERSIDADE FEDERAL DO PARÁ

PPGG